OBSERVATIONS ON PEARLS REPORTEDLY FROM THE PINNIDAE FAMILY (PEN PEARLS)

Nicholas Sturman, Artitaya Homkrajae, Areeya Manustrong, and Nanthaporn Somsa-ard

Pearls of all kinds have been used for decorative purposes throughout history. The majority of these have been nacreous, yet certain non-nacreous pearls have also been sought by connoisseurs. *Pinna* (pen) pearls fall into the latter group. The nature of their non-nacreous structure often results in cracking, and because of stability concerns they are very rarely used in jewelry. Nineteen of the 22 samples from this study, reportedly from Pinnidae family mollusks, show similarities in color as well as external and internal structure. Raman, photoluminescence, and UV-Vis-NIR spectroscopic results are discussed, along with the internal characteristics of pearls likely produced by this mollusk.

Mollusks of the Pinnidae family include the *Atrina* species and the more familiar *Pinna* species such as *Pinna nobilis*, as well as the rarely encountered *Streptopinna* species. Like many mollusks, this bivalve contains several members, including *Atrina vexillum*, *Atrina fragilis*, *Atrina pectinata*, *Atrina maura*, *Pinna bicolor*, *Pinna muricata*, *Pinna rudis*, and *Pinna rugosa* (Wentzell, 2003; Wentzell and Elen, 2005). The 22 pearls discussed herein (see figure 1) were submitted for examination by William Larson (Pala International, Fallbrook, California). They were all referred to as "pen pearls," without any details concerning their recovery or provenance. Pen pearls have seldom been covered in the gemological literature, so the results presented here are intended as a reference for those interested in pearls from this important ocean dweller.

THE MOLLUSK

Bivalve shells from the Pinnidae family share a very characteristic outline, tapering from a broad curved end to a pointed tip (figure 2). This unique form, reminiscent of the quill pens once used as writing tools, gives the shell its name. Sometimes referred to as "fan clams," they average 100 to 600 mm in length, though specimens approaching 800 mm (2.5 feet) have been recorded. Apart from size, another claim to fame for *Pinna nobilis* is that its byssal threads, which anchor the shell in the sand during the mollusk's life, were once woven together to make a fabric known as "sea silk."

The Pinnidae family is widely distributed among the oceans of the world, from the Mediterranean to the Red Sea, the Arabian Gulf, and the Indo-Pacific (from southeastern Africa to Melanesia and New Zealand, extending north to Japan and down to New South Wales). In the Western Hemisphere, these mollusks inhabit American waters around Florida, North Carolina, and Texas, as well as Mexico, the Caribbean, and as far south as Argentina (Strack, 2006). One of the authors' diving adventures in the Arabian Gulf off the coast of Bahrain (Sturman et al., 2010) revealed numerous specimens deeply embedded within the sandy floor, typical of the mollusk's behavior.

A quick glance at most Pinnidae shells shows a clear area of nacre at the pointed end and a less-lustrous portion extending across the curved opposite end. Closer examination reveals that the nacreous portions do not, as a whole, exhibit the obvious classic overlapping nacre structures encountered in other bivalves from the same order (Pterioida). Rather, they show a much finer form of nacre that is more difficult to resolve in most cases, even at high magnification (figure 3). This difference stems from the fact that the nacreous portion is not constructed of concentric layers, but

See end of article for About the Authors and Acknowledgments.
GEMS & GEMOLOGY, Vol. 50, No. 3, pp. 202–215,
http://dx.doi.org/10.5741/GEMS.50.3.202.

Figure 1. These 20 completely non-nacreous pen pearls, from the group of 22 samples in this study, are set against a pen shell displaying both nacreous (left) and non-nacreous areas (right). Photo by Lhapsin Nillapat.

of numerous small prisms arranged around the center (Taburiaux, 1985). Since the family comes from the same order as other nacreous species such as those of *Pinctada* and *Pteria*, it is not surprising that nacre should feature somewhere within the shells' composition. But it is intriguing to see the different degree of coverage, given that the *Pinctada* and *Pteria* species are completely nacreous on their inner shells and clearly display overlapping platelet ridges.

The non-nacreous structure that characterizes the bulk of the shell also shows a wonderful mosaic or cellular pattern (figure 4, left) found in most of the pearls produced by this mollusk. These cells often vary from shell to shell in form, transparency, and internal features. Their appearance relative to location within the shell also appears to vary. In the sample from Thailand, the cells near the lip of the shell contained small pinpoint features, while those toward the center lacked these features (figure 4, center).

The cellular structure is visible because each cell is actually a long thin crystal composed of calcite, as noted in previous studies (Gauthier et al., 1997). This acicular structure is clearly evident in shells where some of the crystals on the edge have been damaged and broken away (figure 4, right). The crystals' transparency often permits strong light to pass along their length, making areas of both shell and pearl semi-translucent to translucent (Sturman, 2007). This columnar structure also leads to frequent crazing or cracking between the cell and the column walls. This is likely exacerbated by the loss of any water content in the materials.

THE PEARLS

Pen pearls occur in various shapes and sizes, and their color usually ranges from black or dark brown to a more yellowish brown or yellowish orange (Strack,

Figure 2. The 22 pearls from this study are shown together with two shells from GIA's Bangkok laboratory reference collection. The lighter-colored Pinna *shell and the darker* Atrina *shell display the distinctive external appearances of mollusks from the Pinnidae family. The more lustrous nacreous structure is seen at the tapered ends. Photo by Lhapsin Nillapat.*

Figure 3. The nacreous structure visible at the pointed end of each pen shell half is not as clearly defined as the nacre in other Pterioida mollusks. Pen shells display a more "linear"-looking nacre. Photo by Artitaya Homkrajae; reflected light, magnified 112.5×.

2006). This range of color was apparent in the samples we studied, where one of the drops stood out from the darker, more typical pearls. Most pearls form as cyst or whole pearls, but some—again in keeping with other mollusks—occur as blister pearls or blisters (figure 5; CIBJO, 2013). Blister pearls and blisters are particularly useful when trying to compare the structure of pearls to their hosts, as they occur together and provide a direct means of comparison. One of the greatest drawbacks of pen pearls, though, is their tendency to crack or craze, a characteristic that significantly hinders their market value. This cracking appears to occur only in the non-nacreous pearls, but unfortunately these specimens are the norm.

Nacreous pen pearls (mainly *Atrina* species) are sometimes encountered in jewelry, though far less often than other types of pearls with more marketable color and greater durability. In recent years, however, pen pearls have become much more sought after as farmers, particularly in Indonesia, have learned to use them as nuclei for a new kind of atypical cultured pearl (Hainschwang, 2010). These atypical bead-cultured pearls can be quite challenging for laboratories to identify, though most present no real issues at the moment.

In Brief

- Like their host mollusks, pen pearls may be wholly nacreous or wholly non-nacreous, depending on the species. Partially nacreous examples may also be encountered.
- The surface structures of the non-nacreous areas show a beautiful cellular structure.
- While microradiography and X-ray computed microtomography (μ-CT) techniques are not required for identification, such examination does reveal the wonderful, often radial and concentric internal structures present within the pearls.

MATERIALS AND METHODS

Twenty loose undrilled pearls, weighing between 2.74 and 20.70 ct and ranging in color from dark

Figure 4. Left: This section of Pinnidae shell from Thailand shows a graduated cellular structure, with finer cells near the lip of the shell and larger cells toward the middle. Center: The structure within the center of each cell also varies. The cells toward the outer part of the shell exhibit minute impurities in their center, while the cells closer to the middle have empty centers. Right: The cause of the cellular pattern is clearly seen in this broken shell segment, which shows the acicular nature of the individual calcite crystals that form the non-nacreous areas. Photos by Nick Sturman; magnified 32× (left and right) and 176× (center).

*Figure 5. This irregularly shaped blister pearl, attached to the interior of a Pinnidae family (*Atrina *species) shell, measures approximately 21.50 × 17.60 mm. Photo by Nicholas Sturman; shell courtesy of Kenneth Scarratt.*

brown to yellow-brown, were analyzed. Two additional samples weighing 2.78 and 5.81 ct (see pearls 19 and 20 in table 1), exhibiting both silver nacreous and brown non-nacreous areas, were also examined. The properties of all 22 samples are listed in table 1.

The pearls' internal structures were examined using a Faxitron CS-100 2D real-time (RTX) microradiography unit (90 kV and 100 mA excitation), and a Procon CT-Mini model X-ray computed microtomography (μ-CT) unit fitted with a Thermo Fisher 8W/90 kV X-ray tube and a Hamamatsu flat-panel sensor detector.

Their composition was analyzed with an inVia Raman microscope equipped with a 514 nm argon-ion laser (Ar^+), which was used to obtain Raman and photoluminescence spectra. The laser was set at 100% power, and spectra were collected using 10 accumulations, with an accumulation time of 10 seconds per scan.

The spectra required to characterize each sample's color were collected in the 200–2500 nm range with a Perkin-Elmer Lambda 950 ultraviolet/visible/near-infrared (UV-Vis-NIR) spectrophotometer using a reflectance accessory fitted with an integrating sphere. The 250–750 nm range is presented here, because this range contains most color-related reflectance features.

The pearls' chemical composition was analyzed using a Thermo X Series II laser ablation–inductively coupled plasma–mass spectrometry (LA-ICP-MS) system equipped with an attached New Wave Research UP-213 laser and an energy-dispersive X-ray fluorescence spectrometry (EDXRF) unit. Microanalytical carbonate standards MACS-1 and MACS-3 from the United States Geological Survey (USGS) were used as the standards for each method.

Photomicrographs of the surface structures were captured with a Nikon SMZ1500 system using various magnifications up to 176×. Other gemological microscopes with magnification ranges between 10× and 60× were also used during the examination of the shells and pearls. Shells from both *Pinna* and *Atrina* species in GIA Bangkok's reference collection were studied to compare their structural similarities with the sample pearls.

The pearls' fluorescence features were also observed under an 8-watt UV lamp with both long-wave (365 nm) and short-wave (254 nm) radiation, as well as a DiamondView unit.

OBSERVATIONS AND RESULTS

External Structure. The pearl samples showed characteristic non-nacreous structure consisting of a network of cells resembling those pictured in figure 4. The actual shape of the cells varied quite markedly, from a pseudo-hexagonal outline to an elongated curved form. Examples of the range of structures can be seen in figures 11–21. Diaphaneity ranged from opaque to semi-

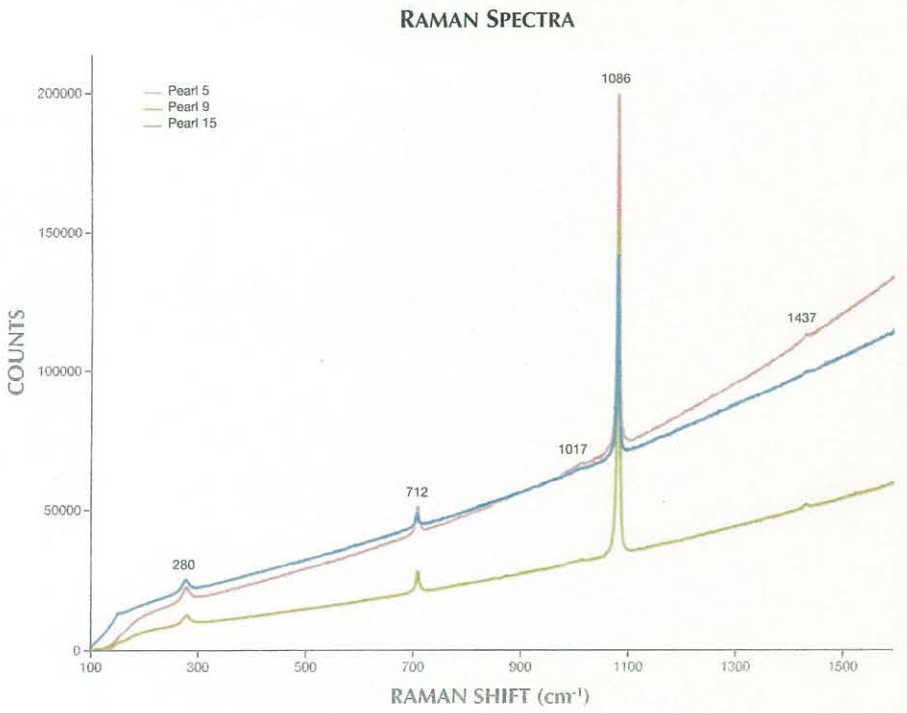

Figure 6. The Raman spectra of pen pearls 5, 9, and 15 show peaks at 280, 712, 1086, and 1437 cm^{-1} (the first two indicative of calcite) and a polyenic-related peak at 1017 cm^{-1}.

translucent, with the lighter-colored samples tending toward the latter (Gauthier et al., 1997; Karampelas et al., 2009). Cracking was very apparent in most of the samples, and some of the cracks were fairly wide and penetrated quite deeply. This is an accepted but undesirable trait encountered in most pen pearls. Using them as nuclei for atypical bead-cultured pearls solves this problem, since the nacre overgrowth hides not just the cracks but the whole pearl.

Samples 19 and 20 were considerably different from the rest of the group. Their shapes were baroque and quite flattened, while their colors were clearly uneven and more bicolored, with silver and brown areas mixed together. Their structure also varied, from a more nacreous type with silver portions to a non-nacreous cellular structure on the brown portions (consistent with the other samples). These two pearls differed in other ways that will be described later in this work.

External Composition. To identify the nature of the minerals forming the pearls, we examined the pearls using the Raman spectrometer with an attached microscope. This analysis showed that the non-nacreous areas consisted of calcite, as evidenced by the peaks at 280 and 712 cm^{-1}, with the associated band at 1086 cm^{-1} (figure 6). The only noticeable exceptions were the spectra for the two bicolored pearls, where the silver nacreous areas produced a slightly different spectrum. Here, the 280 cm^{-1} peak was very weak and accompanied by a series of peaks at 198, 206, 217, and 287 cm^{-1}, while the 712 cm^{-1} peak position shifted to a doublet feature at 701 and 705 cm^{-1}. These features are all characteristic of aragonite, the most common polymorph found in pearls and shells, so we were not surprised to detect it on the more nacreous portions. Previous studies on pearls from *Pinna nobilis* (Gauthier et al., 1997; Karampelas et al., 2009) attributed the cause of color to carotenoids. While we detected the 1017 cm^{-1} peak reported in their studies, the other peaks were not readily apparent, which is unusual. Such pigment peaks exhibit strong resonant phenomena. Their absence could be due to the particular mollusk that produced the pearls or the laser wavelengths used in collecting the spectra, as well as the parameters used to test the samples. No other lasers were used in this study.

Photoluminescence analysis was conducted for samples 5, 9, and 15 (figure 7). The spectra are not identical, as the maxima center is somewhat different on each curve. Yet the overall pattern is quite similar apart from sample 15, the yellow-brown pearl, which has a maximum at approximately 600 nm and is offset slightly to the left of the others. A subtle band at around 700 nm is quite consistent in the samples. Very weak peaks at 555 and 565 nm

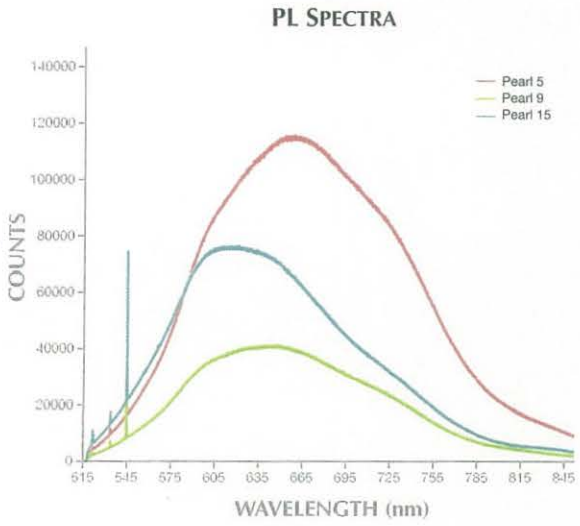

Figure 7. Photoluminescence (PL) spectra of samples 5, 9, and 15 showed different patterns, likely due to the variation in their relative intensities. While the weak feature at around 700 nm stayed consistent, the overall pattern of the peaks varied. The sharp features at 520 and 550 nm are due to the Raman effect.

were observed in the PL spectra. These do not appear to correlate with the polyenic pigment peaks seen around 546 and 558 nm in non-nacreous orange pearls such as Melo pearls, which exhibit polyenic peaks very similar to those stated for pen pearls. Therefore, we believe that polyenic compounds, which belong to the carotenoid family, were not observed in the PL spectra of the samples.

Fluorescence. Reactions to ultraviolet (UV) light were best seen under long-wave UV (LWUV) radiation, where 18 of the pearls exhibited a very weak to moderate chalky yellow fluorescence. Only sample 15 showed a strong chalky yellow of a brighter color. Sample 13 displayed an uneven moderate to strong yellow in the pearl's center, where the color was lighter. Samples 19 and 20 displayed strong chalky yellow reactions on the nacreous areas while the brown non-nacreous patches appeared relatively inert, but closer examination revealed a very weak yellow reaction, in keeping with most of the other pearls. Short-wave UV (SWUV) reactions showed the same colors as LWUV, but with weaker intensity. A few of the pearls that exhibited a very weak reaction to LWUV did not show any clear reaction under SWUV conditions.

To see whether these long- and short-wave reactions were in any way similar, all the samples were examined in the ultra-short UV wavelength (<230 nm) of the DiamondView. The results ranged from a clear bluish reaction to a rather inert reaction, with bluish boundaries between the cellular structure very prominent in most of the images (figures 8 and 9). The strong bluish reaction is a marked change from the yellow reactions the samples tended to ex-

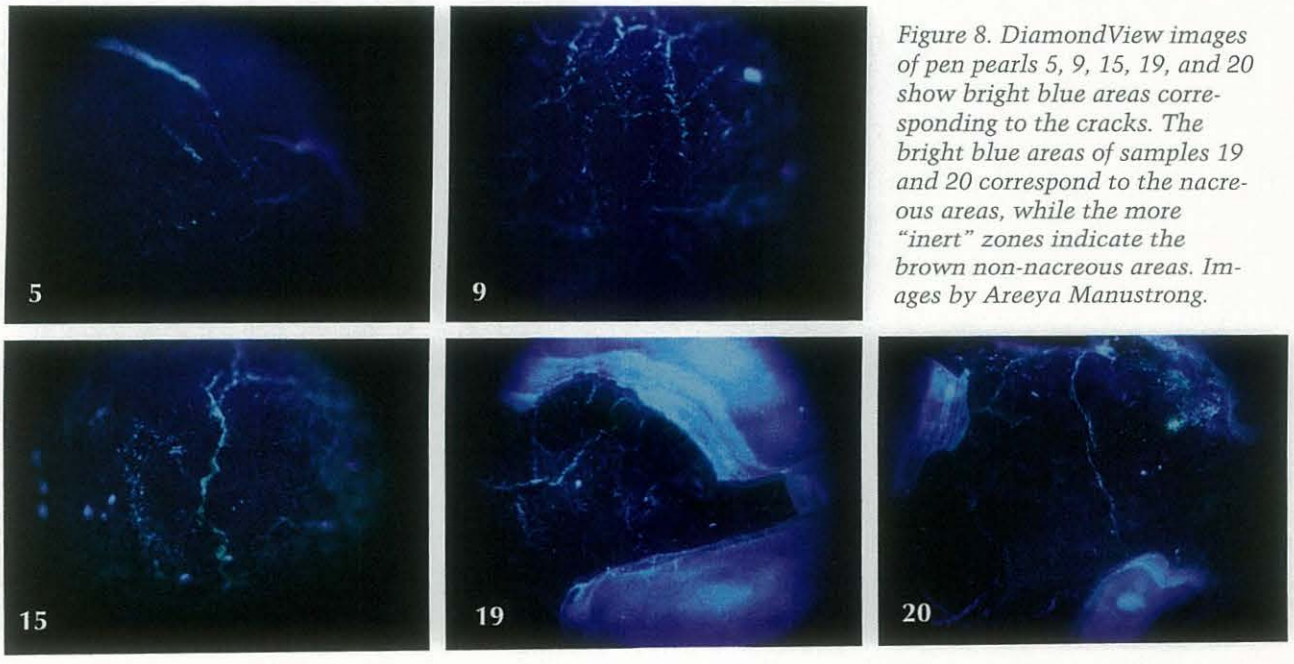

Figure 8. DiamondView images of pen pearls 5, 9, 15, 19, and 20 show bright blue areas corresponding to the cracks. The bright blue areas of samples 19 and 20 correspond to the nacreous areas, while the more "inert" zones indicate the brown non-nacreous areas. Images by Areeya Manustrong.

TABLE 1. Characteristics of the pen pearl samples.

	Pearl sample	Measurement (mm)	Carat weight	Shape	Color
1		8.67 x 8.50 x 8.44	3.65	Drop	Dark brown
2		10.83 x 8.80 x 8.75	4.75	Drop	Graduated brown
3		9.34 x 9.13 x 9.02	5.02	Button	Black
4		8.85 x 8.74 x 8.22	3.92	Button	Brown
5		9.34 x 8.62 x 8.59	4.22	Drop	Black
6		9.09 x 8.65 x 8.61	4.40	Drop	Dark brown
7		8.73 x 8.69 x 7.40	3.78	Button	Dark brown
8		7.49 x 7.46 x 7.27	2.74	Button	Dark brown
9		11.88 x 11.76 x 9.98	8.53	Button	Brown
10		9.16 x 7.51 x 7.48	3.17	Oval	Black
11		14.44 x 10.03 x 9.99	7.99	Drop	Dark brown
12		11.40 x 9.25 x 9.20	6.34	Oval	Dark brown
13		16.58 x 12.05 x 11.93	15.95	Drop	Brown and light brown
14		18.62 x 13.37 x 13.28	20.70	Drop	Black and brown
15		18.07 x 9.40 x 9.32	8.00	Drop	Yellow-brown
16		12.96 x 12.89 x 12.15	11.27	Drop/ Button	Black
17		17.75 x 9.05 x 9.00	9.52	Drop	Brown
18		11.44 x 11.35 x 8.75	7.80	Button	Dark brown
19		12.70 x 9.96 x 5.31	2.98	Baroque	Silver and dark brown
20		17.39 x 12.46 x 5.93	5.81	Baroque	Silver and brown
21		11.42 x 10.42 x 9.83	7.34	Baroque	Dark brown
22		10.38 x 10.27 x 9.69	6.68	Semi-baroque	Black

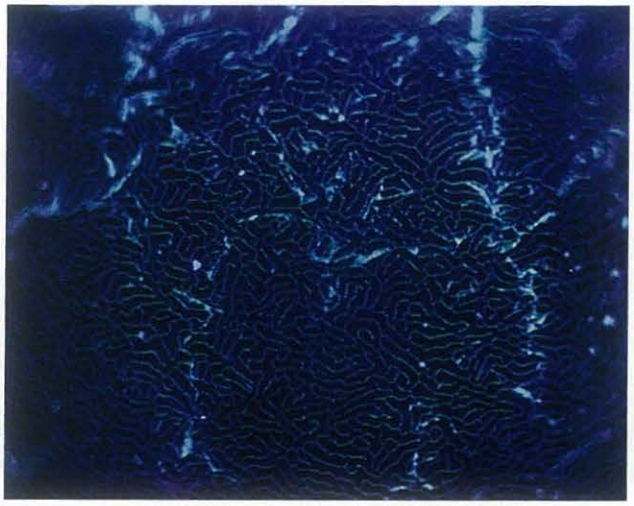

Figure 9. This magnified image of sample 9, as seen in the DiamondView, reveals the wonderful cellular structure in a whole new light. Image by Areeya Manustrong.

hibit under the standard gemological fluorescence unit found in most laboratories.

UV-Vis-NIR Spectrophotometry. While diffuse-reflectance spectra were obtained on all the pearls, only those for the three samples chosen for Raman analysis are shown in figure 10. Despite their differences in color, they showed little variation in the visible part of the electromagnetic spectrum (400–750 nm). Samples 9 and 15 displayed noise in the visible portion that was likely due to their structure and variable translucency, quite different from the more opaque pearls typically tested in the spectrophotometer. Sample 15 did exhibit higher diffuse reflectance than the darker samples, as would be expected for a lighter-colored pearl. All three spectra had a similar reflectance feature in the 320–630 nm range, yet sample 15 had a higher maximum reflectance in the UV region, centered at around 340 nm rather than 330 nm. The shift of this feature and the higher reflectance of the spectrum contributed to the pearl's lighter, more yellow coloration. Sample 5 in particular showed less reflectance and a slightly greater reflectance range. This, together with the approximately 330 nm point of maximum reflectance in the UV region, contributed to its darker appearance.

Chemical Composition. Two methods of chemical analysis were used in this study: EDXRF and LA-ICP-MS. EDXRF, a nondestructive technique, covers a greater sampling area and is more surface-specific. It is widely used by gemological laboratories and provides sufficient data to assist in most identification tasks. It does, however, have relatively high detection limits, and elements lighter than sodium cannot be detected. While the EDXRF results revealed low levels of Mn, consistent with pearls from a saltwater environment (Gutmannsbauer and Hänni, 1994), we wanted to gain a more accurate idea of the quantities of elements present.

We turned to LA-ICP-MS, which examines a smaller micron-sized area of the surface and the underlying material and offers better sensitivity and element coverage. The results confirmed the pearls' known saltwater origin on the basis of low manganese (Mn) levels and the expected results for boron (B), gallium (Ga), and barium (Ba). Strontium (Sr) levels were on average slightly lower than those usually recorded for saltwater mollusks, but still within the saltwater range. While they do not allow a direct comparison with pen pearl chemical composition, data collected from *Pinctada maxima* pearls show some similarities when each element is compared (Scarratt et al, 2012). Li and Fe were present in slightly higher concentrations in the pen pearls. The LA-ICP-MS results for the pen pearls are summarized in table 2.

Figure 10. Samples 5, 9, and 15 showed similar UV-Vis-NIR spectra despite their variation in color. The "noise" in the ultraviolet to visible region (250–750 nm) is likely due to the pearls' structure.

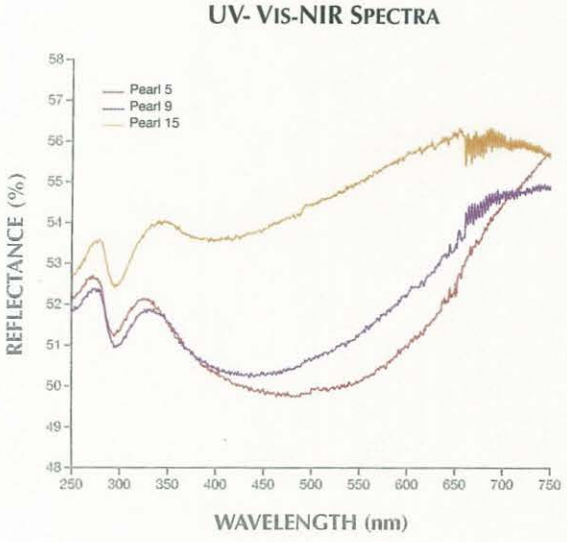

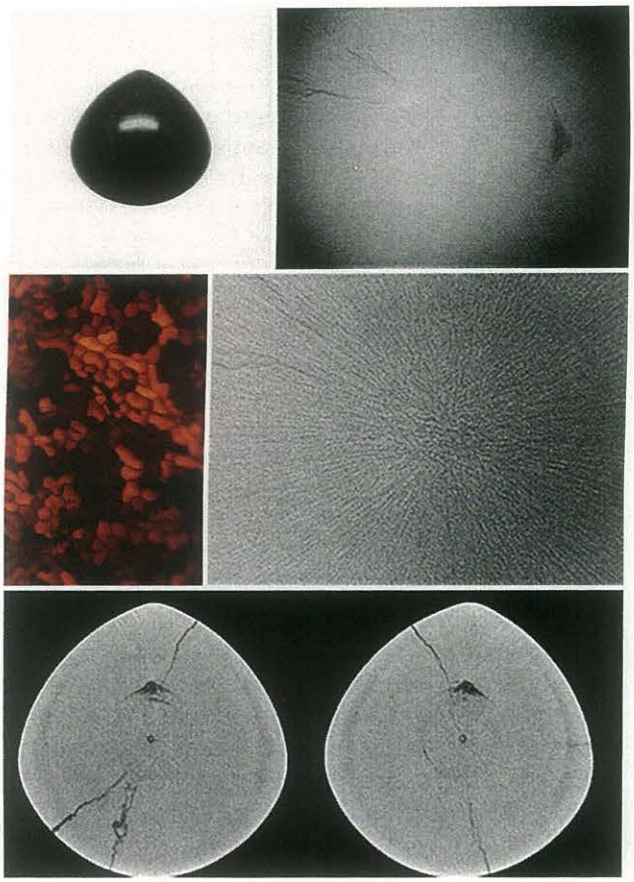

Figure 11. Pen pearl 1's external appearance (top left), microradiographic structure (top right and middle right), surface structure (middle left, magnified 60×), and μ-CT images of two slices (bottom). Photos by Artitaya Homkrajae.

The most significant differences observed between the nacreous and non-nacreous areas in samples 19 and 20 are highlighted by the bold numerals in the table. The most dramatic difference occurred with magnesium (Mg), which showed significantly lower concentrations in the nacreous areas than the non-nacreous areas of all the other pearls. The elemental concentrations in the non-nacreous areas of all 22 samples matched one another well, as would be expected for such similar-looking material. Many more samples of known pen pearls will need to be analyzed to determine whether any correlation exists, yet the detailed chemical analysis of pen pearls is not part of routine laboratory work.

Internal Structure. Viewed in cross-section, the internal structures of non-nacreous pen pearls appear to possess a distinct radial columnar structure. Not surprisingly, this radial structure often manifests itself clearly in microradiographic images, since the path length equals the entire thickness of the sample when exposed to the X-ray source. The clarity is usually not so obvious in the micron-thick slices of CT images. On the other hand, concentric ring structures are often more visible via CT than the RTX method. A selection of the thousands of RTX and CT slice images obtained by the authors appears in figures 11–21. These show that small, dark natural nuclei or cores sometimes exist at the center of the radial and concentric structures, while undesirable cracks also extend to various degrees throughout most of the samples.

Sample 15 exhibits the only atypical internal structure of the completely non-nacreous pearls in this study; it also differs in coloration and diaphaneity, as seen in figure 16. The structure consists of a series of connected voids and what are probably conchiolin-rich chambers that extend from the tapered

Figure 12. Sample 5's external appearance (top left), microradiographic structure (top right and middle right), surface structure (middle left, magnified 60×), and μ-CT images of two slices (bottom). Photos by Artitaya Homkrajae.

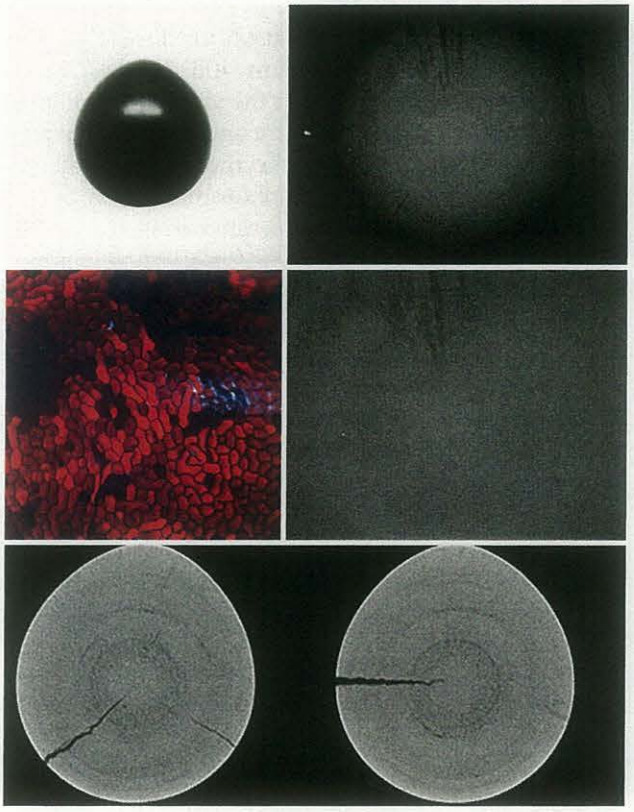

TABLE 2. Trace-element composition obtained by LA-ICP-MS of 22 pen pearls, in parts per million weight (ppmw).

Pearl sample	^{7}Li	^{11}B	^{23}Na	^{24}Mg	^{31}P	^{39}K	^{45}Mn	^{57}Fe	^{69}Ga	^{88}Sr	^{137}Ba
1	2.50	27.84	6222	4803	bdl	242	1.19	264	bdl	946	0.57
2	2.24	2.54	4312	2458	bdl	103	bdl	291	bdl	670	0.51
3	2.61	10.10	5560	3207	bdl	144	2.74	288	bdl	8067	0.74
4	2.49	32.19	5924	3370	bdl	209	1.95	328	bdl	780	0.62
5	2.62	22.43	5674	2795	bdl	213	bdl	304	bdl	798	0.41
6	3.05	15.33	6127	3249	bdl	220	bdl	301	bdl	756	0.43
7	1.92	5.43	5297	3314	39.98	150	1.43	219	bdl	815	0.93
8	1.92	9.92	5016	3395	bdl	129	1.12	264	bdl	749	0.35
9	2.39	23.02	6352	3563	45.07	259	bdl	248	bdl	755	0.29
10	2.31	26.44	5787	4052	bdl	249	0.94	259	bdl	755	1.21
11	2.30	10.33	4902	2907	bdl	143	bdl	269	bdl	714	0.31
12	2.34	12.76	4600	4005	bdl	189	5.86	265	bdl	757	0.28
13	2.19	2.61	4838	3194	bdl	142	1.75	238	bdl	785	1.65
14	4.03	20.86	6792	2947	58.08	291	1.27	261	bdl	842	0.68
15	2.36	17.39	5958	5264	46.97	368	4.44	217	bdl	818	1.33
16	2.50	32.96	6217	3391	bdl	230	3.21	239	bdl	1044	1.09
17	3.04	30.09	6285	4096	40.57	158	1.04	220	bdl	836	0.41
18	2.25	37.72	5452	3412	bdl	114	1.72	271	bdl	529	0.73
19 - Brown	2.49	21.96	7129	3781	bdl	175	1.32	311	bdl	704	0.40
19 - Nacre	**0.96**	2.32	**9806**	**54**	**171**	110	bdl	218	bdl	1016	0.48
20 - Brown	2.52	9.90	6915	5250	bdl	213	1.23	321	bdl	813	0.34
20 - Nacre	**0.59**	9.01	**9170**	**51**	**151**	82	bdl	251	bdl	1030	0.23
21	2.32	17.79	5617	3837	bdl	262	2.80	217	bdl	789	1.45
22	2.37	14.34	6031	3983	bdl	225	0.90	255	bdl	776	0.63
Detection limits	0.25	2.13	11.92	0.70	36.17	5.42	0.80	31.33	0.12	0.11	0.12

Abbreviation: bdl = below detection limit

point toward the broader end. The central irregular nucleus consists of another void/conchiolin-rich area that possesses an internal structure. Given the specimen's size and the lack of commercial culturing of this mollusk, the pearl is almost certainly natural in origin.

Of the 22 pearls examined, samples 19 and 20 are the exceptions to the rule in nearly every way. Not only do they possess non-nacreous and nacreous structures within the same pearl, but the nature of their internal structure is also completely at odds with that of the other samples. Both show a very prominent void-

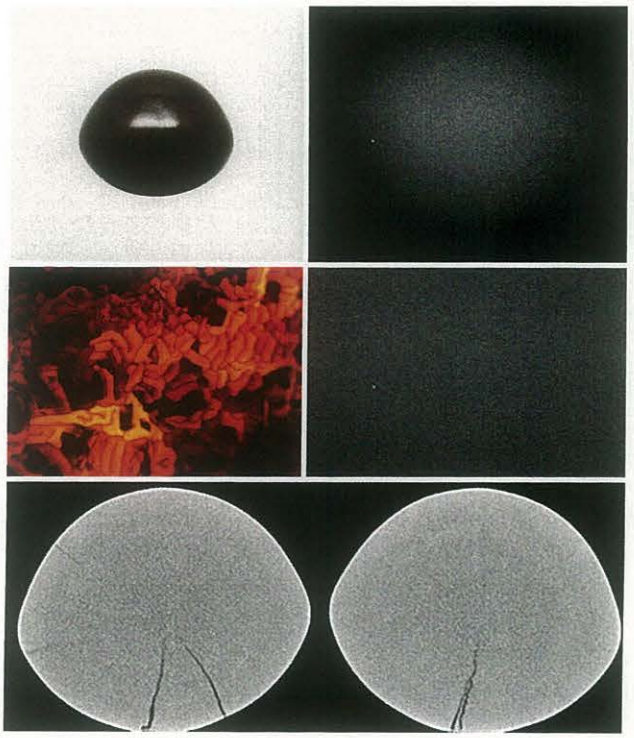

Figure 13. Sample 9's external appearance (top left), microradiographic structure (top right and middle right), surface structure (middle left, magnified 60×), and μ-CT images of two slices (bottom). Photos by Artitaya Homkrajae.

like feature (figures 17–20) in which a few "walls" of what is very likely conchiolin are associated with small white "seeds." These seeds appear to consist of material rich in calcium carbonate, given the similar radio-opacity of the features and their surrounding calcite and aragonite host, as well as the organic nature of the pearls themselves. It is interesting to note that the white seed features are similar to those observed in some non-bead-cultured pearls we have encountered during research on known samples from farms, though similar structures may also be encountered in natural pearls and are not conclusive proof of culture.

It is worth noting that we observed a direct correlation between the structure (solid or hollow) and the specific gravity in these 22 samples. All the solid pearls (samples 1–18, 21, and 22) gave SG values between 2.39 and 2.53; this variation was likely due to the size and depth of the cracks and any air trapped in them during hydrostatic measurements. Samples 19 and 20 again proved the exceptions, with SG values of 1.76 and 2.02, respectively. Given the large voids observed in their structures, this was not surprising.

Culturing and Treatments. While many different mollusks are known to produce cultured pearls, most are bivalves associated with species from the Pteriidae family or various freshwater mollusks from the *Hyriopsis* genus that are frequently used to produce non-bead-cultured, mantle-grown cultured pearls (Farn, 1991; Strack, 2006). Cultivation using mollusks from other families is usually the exception rather than the rule today. The only other mollusks known to produce cultured pearls to any commercial extent are from the *Haliotis* genus and, on rare occasion, the *Strombus gigas* (Queen conch) species. Cultured pearls from the Pinnidae family can be added to the list of those that have undergone trials but without commercial success so far (Landis, 2010).

As with all pearls, the subject of treatments was often at the forefront of our thoughts on these pen pearls. No treatments were detected in this group, nor are the authors aware of any treatment applied to the Pinnidae family. Waxing or some other method could

Figure 14. Sample 11's external appearance (top left), microradiographic structure (top right and middle right), surface structure (middle left, magnified 50×), and μ-CT images of two slices. Photos by Artitaya Homkrajae.

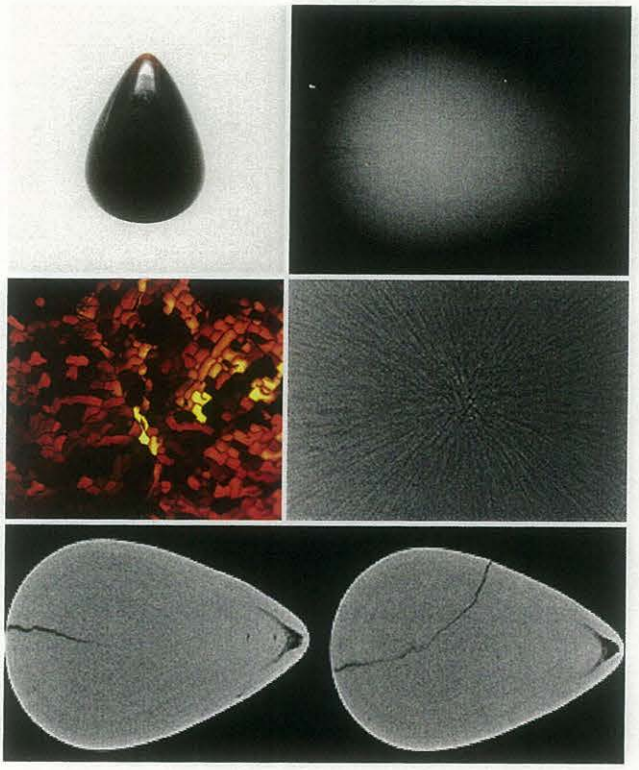

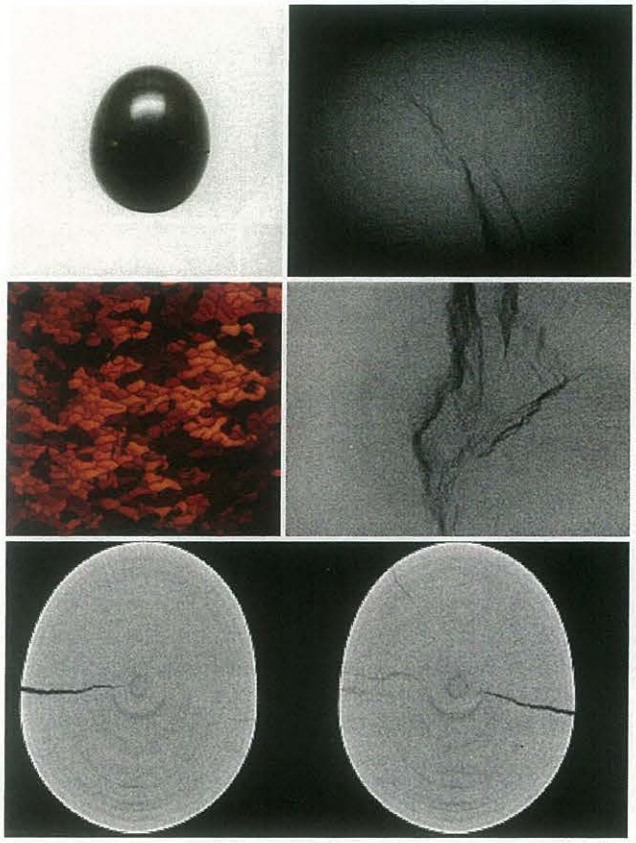

Figure 15. Sample 12's external appearance (top left), microradiographic structure (top right and middle right), surface structure (middle left, magnified 70×), and μ-CT images of two slices (bottom). Photos by Artitaya Homkrajae.

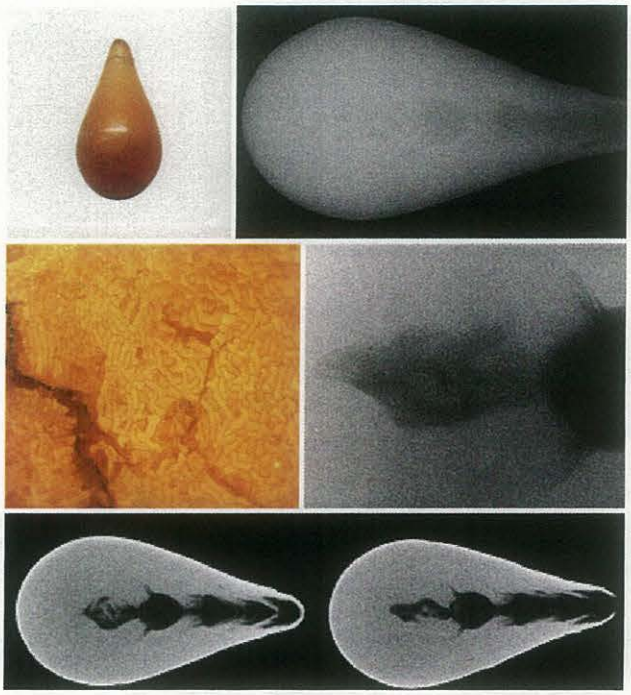

Figure 16. Sample 15's external appearance (top left), microradiographic structure (top right and middle right), surface structure (middle left, magnified 50×), and μ-CT images of two slices (bottom). Photos by Artitaya Homkrajae.

be used to hide cracks or prevent them from expanding and deepening, but no such procedure was observed in this study.

CONCLUSION

Pen pearls are among the least appreciated pearls due to durability issues and their rather plain appearance. Yet they possess one of the most wonderful internal structures of all mollusk creations, and the surface patterns revealed by magnification are truly remarkable works of nature that all pearl aficionados would do well to observe. The columnar structures in their radiating forms produce unique specimens that allow light to be transmitted along their length to varying degrees, causing some pen pearls to appear semi-translucent to the unaided eye. Not many pearls can lay claim to this characteristic.

These radiating concentric structures manifest themselves clearly during examination with direct microradiography and X-ray computed micro-tomography (μ-CT). These techniques also demonstrate that in the 22 samples studied here, the structures do not always conform to the norm. Pen pearls

Figure 17. Sample 19's external appearance (top left), microradiographic structure (top right), and surface structures (bottom, magnified 90× and 112×). Photos by Artitaya Homkrajae.

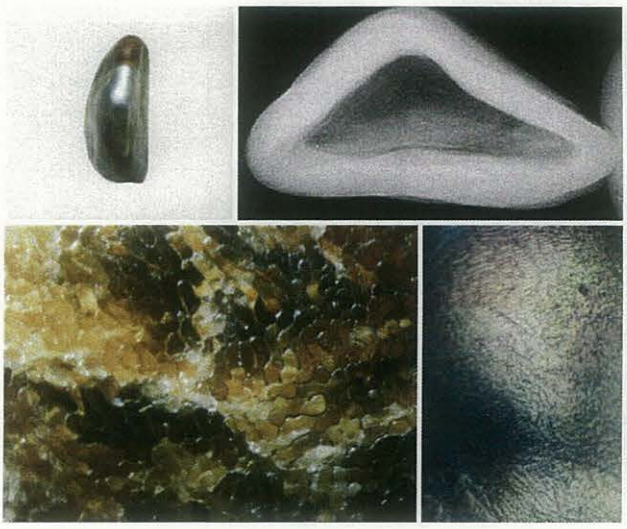

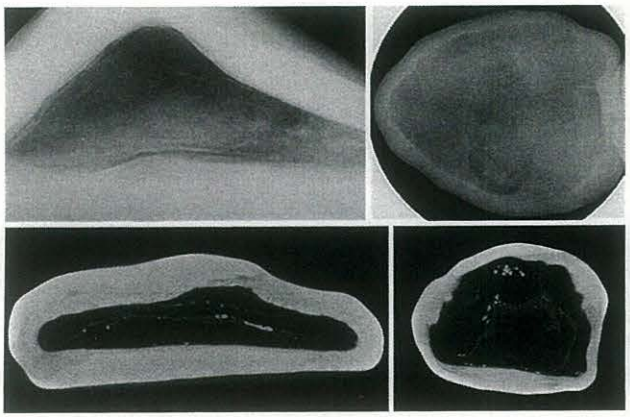

Figure 18. Additional microradiographic images of sample 19 (top) and μ-CT images of two slices (bottom) exhibit some interesting white "seeds" within the void area that are related to internal structural "walls."

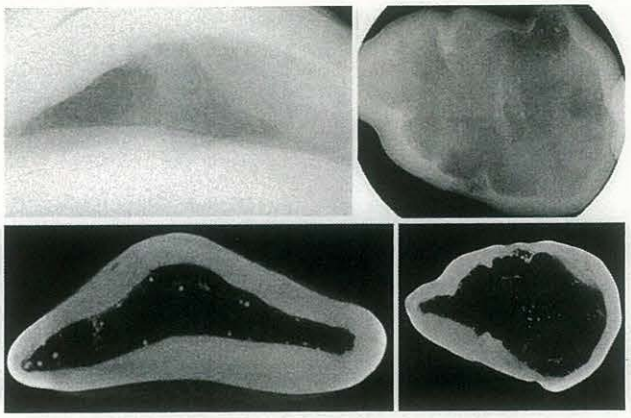

Figure 20. As with sample 19, microradiographic images of sample 20 (top) and μ-CT images of two slices (bottom) show white "seeds" within the void area.

15, 19, and 20 showed void-related features that clearly differed from the other samples examined. The latter two also differed in their external nacreous and non-nacreous appearances, which leads one to question if they are indeed pen pearls. While we cannot be certain, the surface structure seen on the pen shell in figure 4 does bear a close similarity with the features seen in these two examples and in other pearls of reported pen shell origin occasionally examined in the GIA laboratory, so the nature of the nacreous structure appears to support this conclusion. Additionally, the non-nacreous calcitic areas typical of pen pearls are present in both pearls, further supporting the identity. It is noteworthy that both of these pearls, though outwardly different

Figure 19. Sample 20's external appearance (top left), microradiographic structure (top right), and surface structures (lower images, magnified 60× and 112×). Photos by Artitaya Homkrajae.

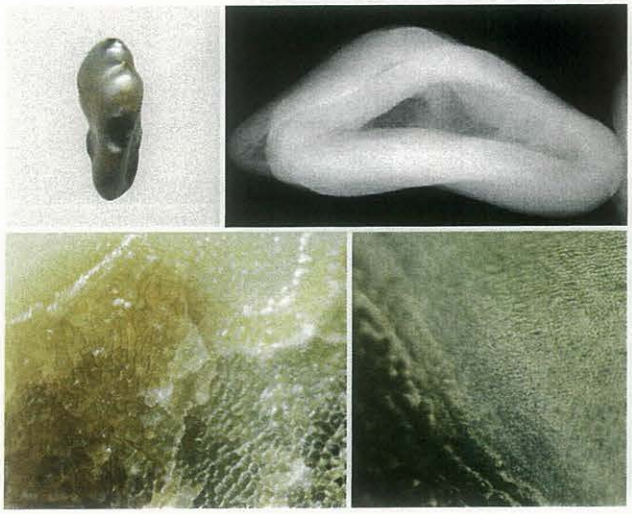

Figure 21. Sample 21's external appearance (top left), microradiographic structure (top right and middle right), surface structure (middle left, magnified 50×), and μ-CT images of two slices (bottom). Photos by Artitaya Homkrajae.

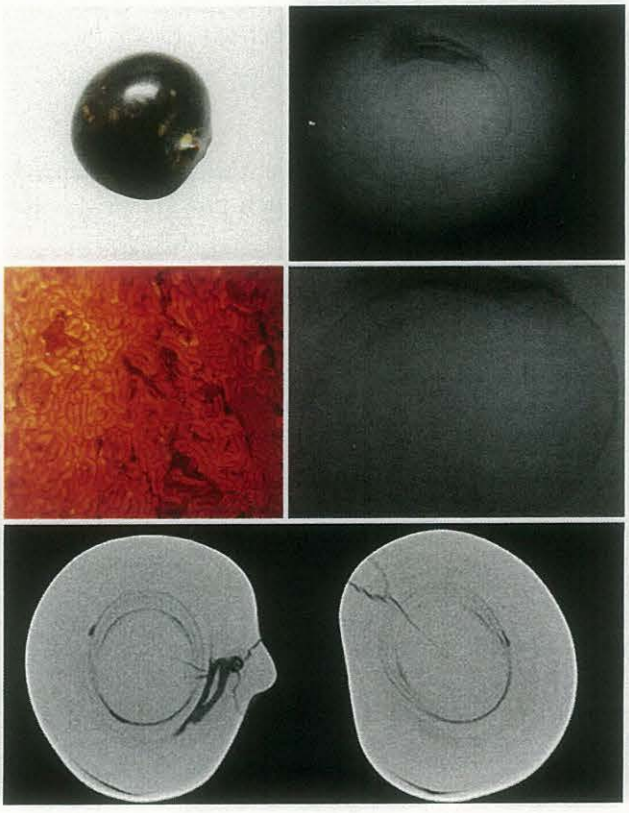

from the other 20 samples, share similar internal characteristics.

This work, along with those previously published by Gauthier et al. (1997) and Karampelas et al. (2009) appear to be the most comprehensive studies on pen pearls to date. Whereas the latter focused on pen pearls from a single known species of Pinnidae, the samples in this study are from unknown species and could come from several different members of the family.

The recent use of pen pearls as atypical nuclei to create natural-looking cores in cultured pearls has stimulated interest in these unusual specimens. The internal structures shown here will also serve as a reference for anyone studying the internal variations in pen pearls.

ABOUT THE AUTHORS

Mr. Sturman (nsturman@gia.edu) is senior manager of pearl identification, Ms. Homkrajae is supervisor of pearl identification, Ms. Manustrong is a staff gemologist, and Ms. Somsa-ard is an analyst, all at GIA's Bangkok laboratory.

ACKNOWLEDGMENTS

The authors would like to thank Mr. William Larson of Pala International in Pala, California, for allowing us to examine the pen pearls. We also thank our colleagues in Bangkok who assisted with this work and the reviewers for their helpful and constructive feedback.

REFERENCES

CIBJO (2013) CIBJO Pearl Blue Book. http://www.cibjo.org/download/13-10-27%20Official%20Pearl%20Book.pdf (date accessed: February 8, 2014).

Farn A. (1991) *Pearls: Natural, Cultured and Imitation*. Butterworth-Heinemann Ltd., Oxford, UK.

Gauthier J.-P., Caseiro J., Lasnier B. (1997) The red pearls of *Pinna nobilis*. *Australian Gemmologist*, Vol. 19, No. 10, pp. 422–426.

Gutmannsbauer W., Hänni H.A. (1994) Structural and chemical investigations on shells and pearls of nacre forming salt- and fresh-water bivalve molluscs. *Journal of Gemmology*, Vol. 24, No. 4, pp. 241–252.

Hainschwang T. (2010) A difficult new type of cultured pearl entering the market. *Gemnotes*, Vol. 1, No. 2, pp. 6–11.

Karampelas S., Gauthier J.-P., Fritsch E. (2009) Gem News International: Characterization of some pearls of the Pinnidae family. *G&G*, Vol. 45, No. 3, pp. 221–223.

Landis B.Y. (2010) Dreams of black pearls, http://younglandis.wordpress.com/2010/04/22/penshellpearls (date accessed: September 8, 2014).

Scarratt K., Bracher P., Bracher M., Attawi A., Safar A., Saeseaw S., Homkrajae A., Sturman N. (2012) Natural pearls from Australian *Pinctada maxima*. *G&G*, Vol. 48, No. 4, pp. 236–261, http://dx.doi.org/10.5741/GEMS.48.4.236.

Strack E. (2006) *Pearls*. Ruhle-Diebener Verlag, Stuttgart, Germany, 707 pp.

Sturman N. (2007) Gem News International: An unusually translucent non-nacreous pearl. *G&G*, Vol. 43, No. 3, pp. 259–260.

Sturman N., Karampelas S., Al-Attawi A., Abduriyim A. (2010) Gem News International: Natural pearl diving off the coast of Bahrain. *G&G*, Vol. 46, No. 4, pp. 318–319.

Taburiaux J. (1985) *Pearls: Their Origin, Treatment & Identification*. Chilton Book Co., Radnor, Pennsylvania.

Wentzell C. (2003) Gem News International: Some interesting pearls from the North American West Coast. *G&G*, Vol. 39, No. 4, pp. 332–334.

Wentzell C., Elen S. (2005) Gem News International: Pen shell pearls—nacreous and non-nacreous. *G&G*, Vol. 41, No. 3, p. 267.